

LASER PARAMETER EFFECTS ON SURFACE QUALITY OF ADDITIVE MANUFACTURED COMPONENTS

S.E. Hoosain^{1*} & L.Tshabalala²

¹ Research and Development, Transnet Engineering, South Africa
Shaik.Hoosain@transnet.net

² National Laser Centre, Council for Scientific and Industrial Research, South Africa
LTshabalala1@csir.co.za

ABSTRACT

In the current study, the selective laser melting process was used to manufacture hollow tubes and solid cubes from Ti6Al4V powders to evaluate the effect of laser parameters on surface finish. Laser power and speeds for the contours, and hatch-contour overlap were varied for evaluation. The samples were then analysed for, wall thickness, porosity and surface roughness with the use of micro x-ray tomography and surface profilometry respectively for comparison. Results show that the best surface finishes are obtained using higher scan speeds and power densities of between 5-6 kW/mm².

¹ The author was graduated M Eng (Metallurgy) degree in the Department of Metallurgy and Materials Engineering, University of Witwatersrand

² The author was graduated D Tech (Engineering Metallurgy) degree in the Department of Chemical & Metallurgical Engineering, Tshwane University of Technology

*Corresponding author

1. INTRODUCTION

Additive manufacturing (AM) or 3D printing complements conventional manufacturing techniques by providing another option utilising a layer by layer build approach [1-3]. This technique for metals, predominantly uses powder or wire as the feedstock material which is selectively melted using a focused heat source i.e. laser or electron beam, which is then consolidated upon cooling to form a part [2]. One of the inherent advantages of AM is that it allows the design of complex parts as AM has significantly less manufacturing constraints than traditional CNC manufacturing processes. Further advantages include the continued lower capital costs, reduced part count since a single consolidated part can be manufactured, easy product revisions, reduction in waste and energy as well as flexibility in choice of material to use. Additive manufacturing of metals still has drawbacks that require careful process control: the high temperature gradients and densification ratio during the process yield high internal stresses which can lead to part distortion; the risk of balling and dross formation in the melt-pool may result in poor surface finish [3]. Additive manufactured parts generally have poorer mechanical properties than the equivalent wrought material and are typically prone to defects such as voids or porosity, which negatively affect their mechanical performance. Defects should be minimized in size and extent, which can be achieved through process parameter optimization [4,10].

Density, porosity and surface roughness metrology can play an enabling role in AM manufacture and research as a means of gaining further understanding of the physical phenomena taking place during the AM manufacturing process [4,5]. Surface conditions of components are prone to surface crack initiation resulting in premature failure. Surface roughness or finish can affect fatigue, mating and sealing surfaces, and geometrical tolerances of parts due to the presence of asperities. The surface finish depends on powder particle size, laser parameters, layer thickness and the orientation of surfaces relative to the build plate. [4-5]. From the literature survey there are a number of parameters in the AM process that can be controlled to improve the surface finish [7-9]. Laser power determines the temperature gradient leading to melting and re-melting of the powder and previous layers which significantly affects the surface finish. Interaction time between the heat source and the metal also determines the total energy input during processing which leads to variations in surface quality in terms of roughness. A hypothesis proposed is that larger melt-pools can drag semi-molten particles from adjacent areas into the melt-pool and become embedded in the edge of the track surface contributing to an increase in roughness. This would occur at slower scan speeds. Orientation of the part layout and layer thickness can lead to the stair step effect which can result in poor surface quality [8-9]. The hatch distance has also been found to affect the surface roughness of parts [9].

The contours which define the edge of every consolidated layer and ultimately the properties of the external surfaces of any part that is produced by the SLM (Selective Laser Melting) method. Contours follow the edges of the part, melting along free surfaces of the part geometry. The wall thickness of the contour scans becomes an important variable as this determines the appropriate hatch-contour overlap to use. According to Calignano et al. [3], narrower melt-pools lead to better surface finish which also leads to the desire for narrower wall thicknesses. Contour scans are done in SLM to improve the surface finish of components [10].

The focus of this study is to determine the effects of laser processing parameters on the as-built surface condition and quality of AM samples using the surface response method.

2. METHOD

The experiments were set up on the custom-built selective laser melting platform within an inert glovebox enclosure. The laser used was a 5kW IPG YLS 5000 ytterbium fibre laser with a wavelength of 1076 nm and a delivery fibre core diameter of 50 μm . The scanner used was

an Intelliweld 30 FC V system. Materials used were Ti6Al4V, gas atomized with particle size distribution of 20-60 μm supplied by TLS Technik GmbH & Co. (Germany). The high power Aeroswift operating parameters were varied to achieve power densities ranging from 3 to 6.5 kW/mm^2 with consolidation rate of up to 20 m/s at fixed layer thickness of 50 μm . The samples built were 10 mm x 10 mm x 15 mm hollow square tubes to investigate the effect of power density and consolidation rate on surface quality and 10mm solid cubes to investigate the effects of the contour-hatch overlap on the surface finish. Figure 1 shows the custom designed and built glovebox.



Figure 1: Image of the custom designed and built glovebox

2.1 Hollow samples

The qualitative criteria for elimination of the samples produced was the “light test” to identify the porous samples (insufficient densification) for elimination. A light was shined onto the thin wall and any see-through effects meant a large degree of porosity. The remaining samples were then subject to visual inspection for defects and from these remaining samples wall thickness measurements were done using a Vernier caliper. As smaller wall thicknesses would implicitly mean narrower melt-pools, the aim would be to aim for laser parameters leading to smaller wall thicknesses to support the hypothesis mentioned. Mechanical roughness profilometry measurements tests were done using a Mahrsurf PS1 profilometer according to the ISO 4287 standard using a calibrated standard with a 4.8mm sampling length on the subsequent samples. The parameter for the best surface finish was then taken for the subsequent experiments in section 2.2.

Design of Experiments (DOE) was used to reduce the number of experiments to obtain the maximum optimum conditions. Response Surface Methodology (RSM) correlates the relationships between the primary variables and one or more output response variables. The purpose of the analysis of variance (ANOVA) is to investigate significant forming parameters that affect the wall thickness of the contour to produce improved the surface finish of the parts.

The parameters were modelled using the response surface method. This design consists of a complete 2k factorial design, where k is the number of variables whose factors level are coded as -1 and 1. The factors and levels used in the factorial design were given in table 1.

Table 1: Factors and levels used in factorial design

Parameters	Units	Min	Max	Coded Low	Coded High	Std. Dev.
Power density (A)	kW/mm^2	3	6.5	-1 (3.00)	+1 (6.50)	1.212
Interaction time (B)	s	50	175	-1 (50.0)	+1 (175.0)	43.30
Consolidation rate (C)	mm/s	5.7	20	-1 (5.7)	+1 (20.0)	

Design Expert provides prediction equations in terms of actual units and coded units. The coded equations are determined first, and the actual equations are derived from the coded equations. The quantitative criteria were derived to get the actual equation with each of the terms in the coded equation is replaced with its coding formula.

2.2 Solid cubes

The 10mm solid cubes were built using different contour - hatch overlaps of 0 %, 30 %, 50 %, 70 % (70% being the closest distance between the contour and hatch centres) with parameters taken from the contour conditions of the aforementioned hollow tube experiments. The solid cube samples were analysed for porosity and surface roughness by Micro-Xray tomography (micro-CT) and mechanical profilometry. Micro-CT) was performed using a standard laboratory micro-CT system with scan settings of 200 kV, 70 μ A, with 0.5 mm beam filter with image acquisition of 500 ms per image, 2400 step positions in a full 360 degree rotation were used. The data was then analysed in Volume Graphics VGStudioMax 3.1. The image processing works by including all material and air (closed pores) [10]. For surface topography measurement via micro-CT, an average line is fitted using two points on the surface. Along this line, at discrete points over the entire distance, a deviation distance is calculated for the actual surface vs the line. This deviation is the actual distance from the line, the average of these deviations will be the Ra value. Mechanical roughness profilometry measurements were performed on the solid cubes using the aforementioned method and equipment. Results reported are Ra (mean roughness). Due to IP concerns only general parameters in table 2 of some of the remaining samples after the light test and visual examinations are shown:

Table 2: Summary of parameters of remaining samples

Sample #	Power Density (kW/mm ²)	Consolidation rate (mm/s)
5	3.0	5.71
6	3.0	6.67
9	3.7	10.00
15	4.4	10.00
19	5.1	20.00
21	5.1	10.00
25	5.8	20.00
26	5.8	13.33
31	6.5	20.00

3. RESULTS AND DISCUSSION

Figure 2 shows the as-built hollow square tubes. Visual inspection showed that samples 28, 29, 30 and 34, 35, 36 (as marked in the image) did not consolidate on the base plate and thus delaminated before the build was complete. These samples had lower consolidation rates and higher power densities. This can indicate an unstable melt-pool and a large degree of spatter due to the higher powers and lower speeds [3,11].



Figure 2: Titanium tubes as built. The blue square shows the delaminated samples of poor quality

3.1 Effect of laser parameters on wall thickness

The obtained ANOVA for response surface models are tabulated in table 3. The quality of the fitted model was given by the coefficient measured from the amount of variation around the mean of the model (R-squared). This gives the proportion of the total variation in the predicted response and a high R-squared is desirable (close to 1). Considering the adjusted R-squared (Adj. R²) of 40.28 %, demonstrates that the model is well fitted. Model terms were evaluated by the F-probability value with 95 % confidence level. The P-values were used to check the significance of each coefficient. The P-values less than 0.05 indicates that the model and model terms were statistically significant. In case of wall thickness, the model F-value of 8.42, there is only a 0.03 % chance that the F-value this large could occur due to noise. The Adequate Precision signal the noise ratio, the model ratio of 15.201 which is well above 4, indicated adequate signals to use this model to navigate the design space.

Based on figure 3, the correlation response equation for wall thickness with respect to the input parameters in terms of coded factors are given by the following equation (2). The equation in terms of coded factors predicts the response for the given levels of each factor, by default, the high levels are coded as +1 and low levels as -1. The coded equation is used for identifying the relative impact of the factor by comparing the factor coefficients.

Coded Equation:

$$\sqrt{\text{wall thickness}} = 0.4425 - 0.2507A - 0.0918B - 0.1824AB \quad (1)$$

The model is therefore represented in "coded" terms which fall within the range -1 to +1. The values in the range of the studied parameters that correspond to -1 and +1 are shown in able 1. Their corresponding units are also shown. Where A is in kW/mm² and B is in seconds. However, since the model is in coded terms, to use this model equation, the corresponding coded values (-1 and +1) must be used, not the actual values of the parameters.

Table 3 ANOVA for Response Surface Quadratic Model (response: wall thickness in mm)

Source	Sum of Squares	df	Mean	F-value	p-value	
Block	0.79433	2	0.39717			
Model	0.44988	3	0.14996	8.42018	0.000329	significant
A-Power density	0.14909	1	0.14909	8.37114	0.007036	
B-Interaction time	0.12070	1	0.12070	6.77716	0.014216	
AB	0.25650	1	0.25650	14.4025	0.000668	
Residual	0.53429	30	0.01781			
Cor Total	1.77850	35				
Std. Dev.	0.1335		R ²	0.4571		
Mean	0.4454		Adjusted R ²	0.4028		
C.V. %	29.96		Predicted R ²	0.2161		
			Adeq Precision	15.2012		

Figure 4 shows the graph for wall thickness experimental measurements plotted against the predicted values. Most of the points are well distributed and closer to the straight line ($R^2 = 45.71\%$) which gives the relationship between the experimental and predicted values. The interaction response surface plots are the graphical representation useful to understand interaction properties between the input and output parameters. The ultimate aim of the plot is to predict the optimum values of the variables such that the responses is maximized or minimized. From the analysis of the interaction graphs, the major parameters that influence wall thickness is power density. As mentioned a hypothesis proposed is that larger melt-pools can drag semi-molten particles from adjacent areas into the melt-pool and become embedded in the edge of the track surface contributing to an increase in roughness. Based on the results from figure 4 an optimum power density should be in the region of 5.1 to 5.8 kW/mm². Wall thickness affects the subsequent hatch-contour overlap and serves as a guide to the appropriate spacing.

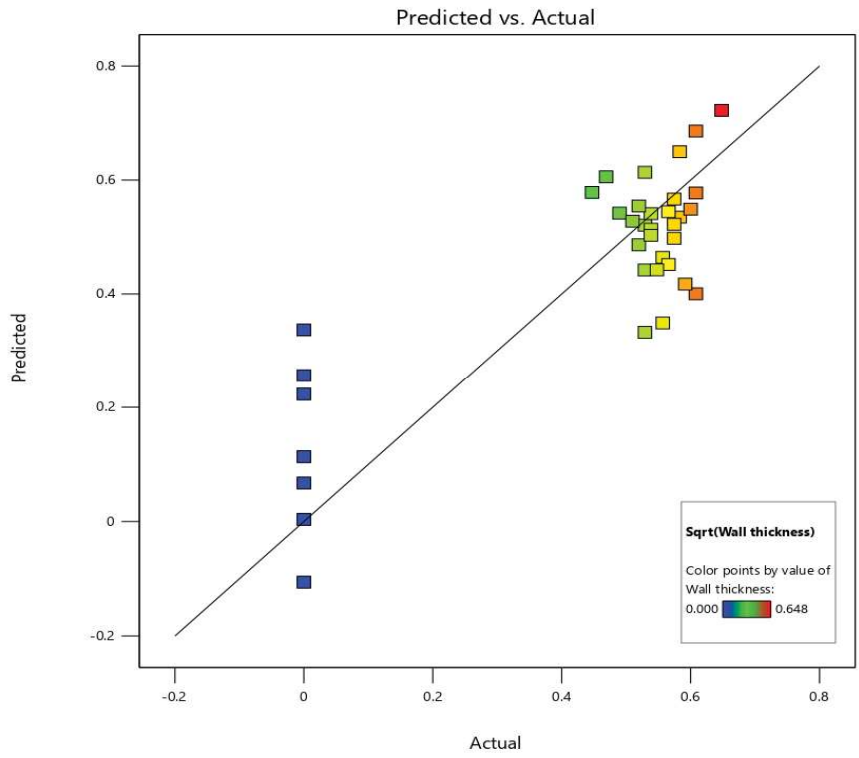


Figure 3: Plot for experimental and predicted responses points to validate the model

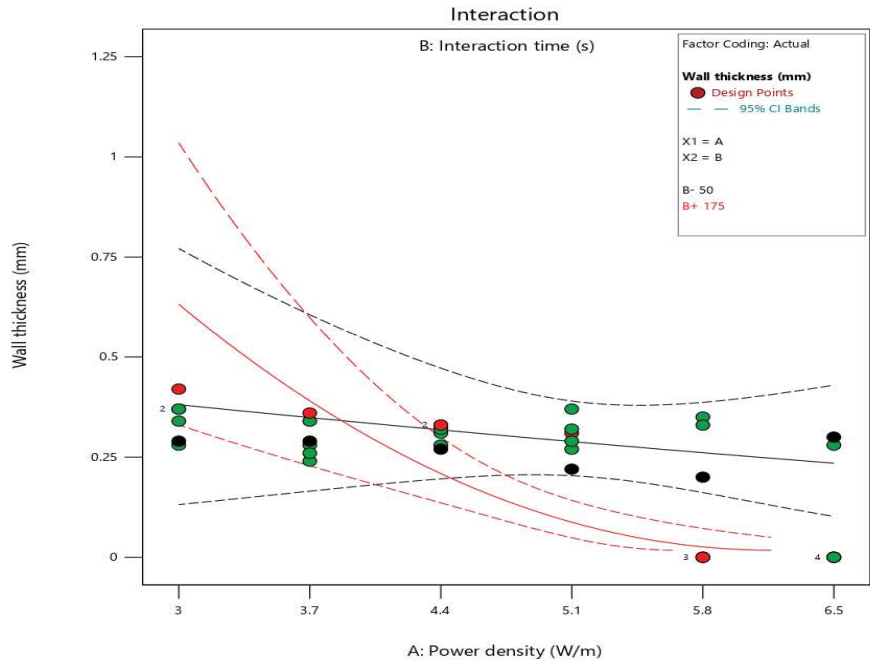


Figure 4: Response surface plot for wall thickness.

3.2 Laser parameter effects on surface roughness

At lower interaction times at power densities of 5.8 kW/mm², the samples produced have poor top surface edge quality showing rough and jagged edges. There are many theories on the effects of the process parameters on surface finish. According to Calignano et al. [3] low scan speeds could increase the volume of liquid produced within the melt-pool; this tends to widen the melt-pool provoking a larger thermal difference and consequently a greater variation of surface tensions. Attempting to reduce these changes in thermal difference and surface tension, the melt-pool may break off into smaller entities, well known as “balling,” which solidify at the edge of the melt-pool increasing surface roughness. Varying the power density below or above the window of 5.1 to 5.8kW/mm² can lead to unstable melt-pools (>5.8kW/mm²) causing spatter or un-melted particles (<k5W/mm²) both leading to poor surface finishes assuming a constant consolidation rate.

After the visual inspection and the “light test”, the samples considered for further analysis include were 5, 6, 9, 15, 19, 21, 25, 26, and 31. These samples correlated to the predicted optimal conditions from the DOE analysis.

These nine samples were then subject to roughness profilometry measurements. Figure 5 shows the surface profile for sample 25 showing an average peak profile for calculating Ra. Table 4 shows the Ra measurements for the selected samples.

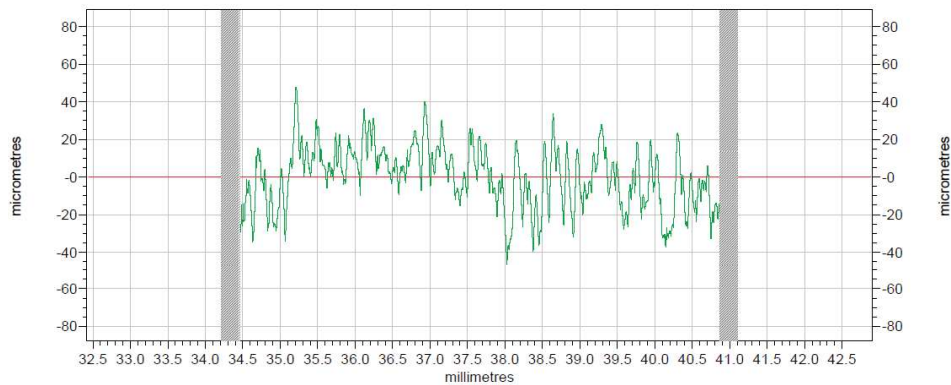


Figure 5: Surface finish profile of sample 25 showing an average line fitted for calculating the mean roughness (Ra)

Table 4 Roughness (Ra) results

Sample #	Power Density (kW/mm ²)	Consolidation rate (mm/s)	Ra
5	3.0	5.71	14.77 ± 2
6	3.0	6.67	13.62 ± 4
9	3.7	10.00	13.52 ± 3
15	4.4	10.00	13.61 ± 3
19	5.1	20.00	13.53 ± 2
21	5.1	10.00	13.75 ± 3
25	5.8	20.00	12.64 ± 2
26	5.8	13.33	14.45 ± 2
31	6.5	20.00	14.07 ± 3

The results generally show that higher consolidation rates obtained better surface finishes. This result agrees with the results of Fallah et al. [11] that an increase of the scanning speed can improve the surface finish (at optimum power). According to Calignano et al. [3], higher speeds would also lead to smaller and narrower melt pools thus giving favourable surface

finishes. As previously stated, a hypothesis proposed is that larger melt-pools can drag semi-molten particles from adjacent areas into the melt-pool and become embedded in the edge of the track surface contributing to an increase in roughness. Based on the optimum power density window derived from figure 4 (5.1 to 5.8kW/mm²) it correlates to the literature [3] and the hypothesis. From these tests sample 25 parameter set was selected for the subsequent testing as it showed minimum surface roughness of $12.64 \pm 2 \mu\text{m Ra}$.

3.3 Effect of hatch-contour overlap on surface roughness and porosity

Contour-hatch overlaps are implemented for geometrical and surface finish considerations. The porosity measurement obtained from micro-CT data only considers closed porosity and that large open pores to the surface are seen as exterior. The porosities measured and analysed from the micro-CT data are shown in table 2. Figure 6 shows the micro-CT image of the cube sample showing a quality view of the surface finish.

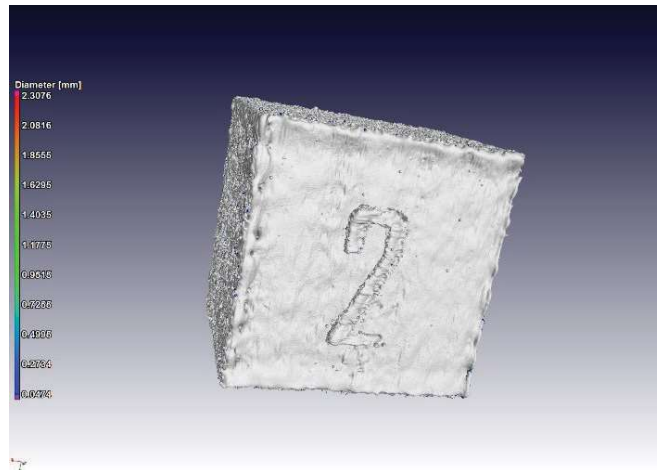


Figure 6: Micro-CT image of sample 2 showing the general geometry and some surface features

Table 5: Porosity results

Sample	Contour-hatch overlap, %	Micro-CT Porosity %
1	0 (no contour)	0.10
2	30	0.35
3	50	0.23
4	70	0.18

Table 5 shows that an increase in the hatch-contour overlap (the contour scan gets closer to the hatch) porosity is decreased. The samples are nearly fully dense ranging from 99.9% to 99.65%. The results indicate that surface porosity was introduced by the contour scans and at 70% overlap between the hatch and contour the porosity was reduced to 0.18%. Figure 7 indicates porosity near the surface as a result of the controlled contour scans and confirms most of the porosity is found near the surface of the sample which is the region of interest for these tests as only the contour scan parameters (overlaps) were varied.

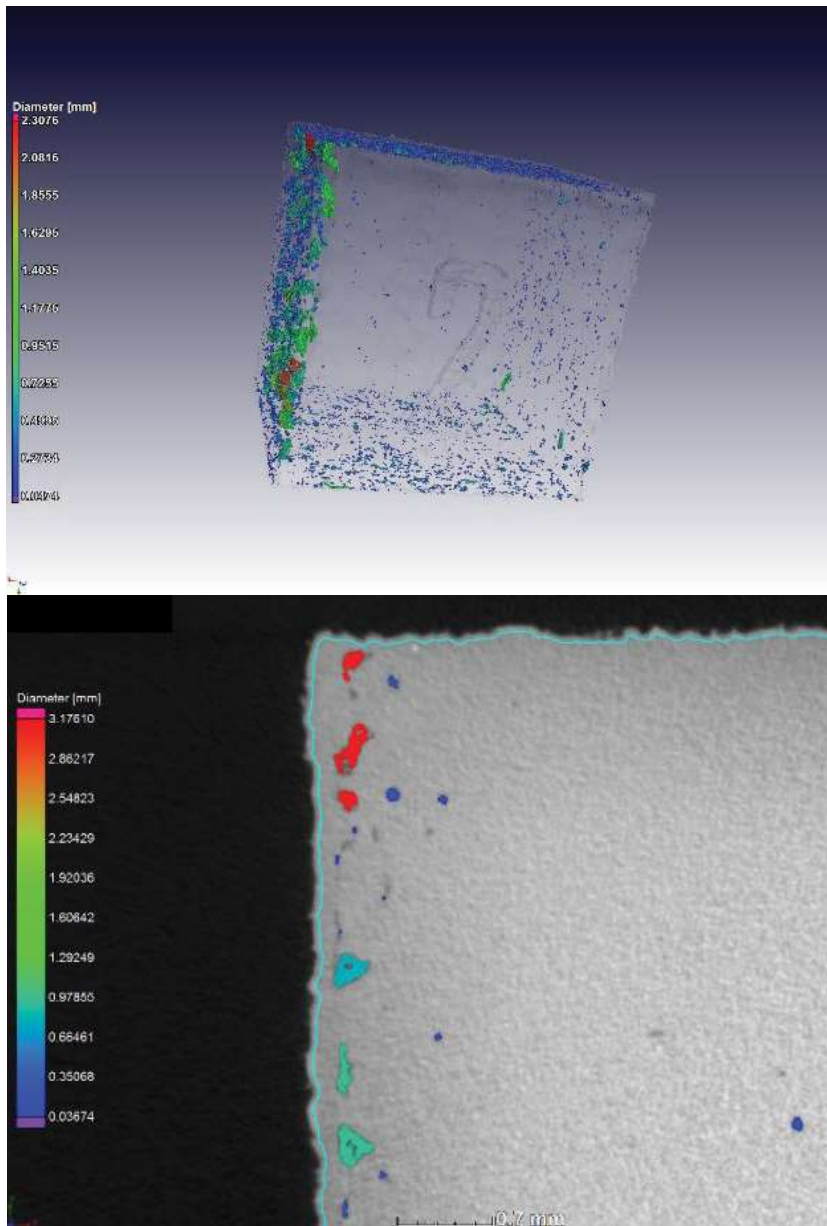


Figure 7: Sliced Micro-CT images representative of the sample 2. The coloured markings show porosity concentrated near the surface

Figure 8 shows the image of sample 2 and sample 4 superimposed - sample 4 is visible as grey values while sample 2 is transparent but shows only the surface as a bright white line (arrow). Clearly the bright white line is less rough than the sample 4 surface. The surface finish results are shown in table 5.

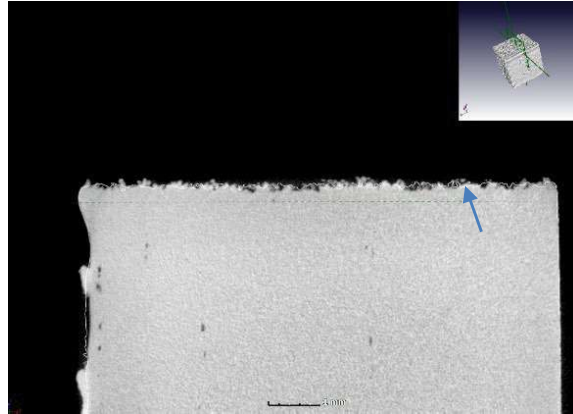


Figure 8: Surface roughness line for samples 2 superimposed.

Table 6: Surface roughness results

Sample	Contour-hatch overlap, %	Profilometer Ra, μm	Micro-CT Ra, μm
1	0 (no contour)	20.88	45.92
2	30	11.54	21.57
3	50	12.85	29.37
4	70	14.74	34.65

As shown in table 6, if the contour is too close to the hatch, more attachments on the contour can be found with the effect of the hatch “shining through” becoming evident [11-12]. The further the distance between the contour and the hatch, a decrease in roughness is observed at the expense of higher porosity near the surface (table 5). As observed, the micro-CT value is higher than the tactile probe values. This can be in part due to the resolution limits of the micro-CT ($10\mu\text{m}$). One contributing reason for the higher micro-CT value is also the additional deep open surface porosity seen by micro-CT which is missed by tactile probe or optical methods. The micro-CT is thus sensitive to such deviations. From the results it shows that the use of contour parameter 25 significantly improves the surface finish of the AM sample. By implementing an appropriate contour-hatch overlap further improvements can be achieved at the expense of an increase in sub-surface porosity.

4. CONCLUSIONS

A contour scanning strategy varying laser power density and laser consolidation rates was utilised as a method to improve the surface finish of as-built AM samples. The trend shows that samples with higher consolidation rates and $5\text{-}6\text{kW}/\text{mm}^2$ power densities have better surface finish. Based on the hypothesis proposed these power densities resulted in smaller wall thicknesses and the higher scan speeds also lead to narrower melt-pools which contributes to an improved surface finish [3]. The optimal contour parameter gave minimum surface finish of 12.64 ± 2 Ra. Although still high it represents a significant improvement. Future work could include lower layer thickness to further improve the surface finish. Lower hatch-contour overlaps (30%) produced better surface finishes with higher porosity just below the surface. The implementation of the contour scans significantly improved surface finish regardless of the degree of overlap.

REFERENCES

- [1] W. J. Sames, F. A. List, S. Pannala, R. R. Dehoff & S. S. Babu. The metallurgy and processing science of metal additive manufacturing. *International Materials Reviews*. Volume 61, 2016, pp 315-360.
- [2] D. Herzog, V. Seyda, E. Wycisk, C. Emmelmann. Additive manufacturing of metals. *Acta Materialia* Volume 117, 2016, pp 371-392.
- [3] F. Calignano, D. Manfredi, E. P. Ambrosio, L. Iuliano & P. Fino. Influence of process parameters on surface roughness of aluminum parts produced by DMLS. *International Journal of Advanced Manufacturing Technologies* Volume 67, 2013, pp 2743-2751.
- [4] A. Townsend, N. Seninb, L. Blunt, R.K. Leach, J.S. Taylor. "Surface texture metrology for metal additive manufacturing: a review." *Precision Engineering* Volume 46, 2016, pp 34-47.
- [5] A. du Plessis, M. Meincken, T. Seifert. "Quantitative Determination of Density and Mass of Polymeric Materials Using Microfocus Computed Tomography." *J Non destruct Eval* Volume 32, 2013 pp 413-417.
- [6] G. Kerckhofs, G. Pyka, M. Moesen, S. Van Bael, J. Schrooten and M. Wevers. "High-Resolution Microfocus X-Ray Computed Tomography for 3D Surface Roughness Measurements of Additive Manufactured Porous Materials." *Advanced Engineering Materials* Volume 3, 2013, pp 153-158.
- [7] Strano, G., et al., Surface roughness analysis, modelling and prediction in selective laser melting. *Journal of Materials Processing Technology*, 2013. 213(4): p. 589-597.
- [8] Gong, H., et al., Analysis of defect generation in Ti-6Al-4V parts made using powder bed fusion additive manufacturing processes. *Additive Manufacturing*, 2014. 1: p. 87-98.
- [9] Hoosain, S.E. Development of contour scanning parameters to improve surface finish in Additive Manufacturing. The 2017 Aeronautical Society of South Africa Conference, 24-26 October 2017, CSIR ICC, Pretoria, South Africa.
- [10] Meiners, W., A. Gasser, and K. Wissenbach, Device and method for the preparation of building components from a combination of materials. 2005, Google Patents.
- [11] A. du Plessis. Standard method for microCT-based additive manufacturing quality control: surface roughness.
- [12] Fallah, Vahid & Iravani-Tabrizipour, Mehrdad & Khajepour, Amir. (2012). Surface finish in laser solid freeform fabrication of an AISI 303L stainless steel thin wall. *Journal of Materials Processing Technology*. 212. 113-119. 10.1016/j.jmatprotec.2011.08.012.
- [13] A.B. Spierings and M. Schneider. Comparison of density measurement techniques for additive manufactured metallic parts. *Rapid Prototyping Journal*. Volume 17/5, 2011, pp380-386.